Smart compact lenses integrating loop-antenna for optics and autonomous micro-energy harvesting for advanced photonic systems

Patrice Salzenstein [1], Blandine Guichardaz [1], Aya Maroua Bessou [1], Laurine Salzenstein [2]
[1] Centre National de la Recherche Scientifique (CNRS), FEMTO-ST Institute, Université Marie et Louis Pasteur (UMLP), 15B avenue des Montboucons, F25030 Besançon Cedex, FRANCE
[2] Information Technology (IT) Department, Université Marie et Louis Pasteur (UMLP), F25000 Besançon Cedex, FRANCE
e-mail: *patrice.salzenstein@cnrs.fr , blandine.guichardaz@femto-st.fr , bessouayamaroua@gmail.com , laurine.salzenstein@gmail.com*

ABSTRACT

We present our investigation in compact smart contact lenses integrating optimized 1 GHz loop antennas with possible autonomous micro-energy sources based on tear-salinity gradients or blinking-induced mechanical harvesting. Building on our previous system-level integration studies and antenna investigations, this work focus on antennas, low-power sensing, and transparent, biocompatible micro battery structures. The approach ensures electromagnetic efficiency, optical clarity, and compatibility with soft-lens manufacturing. These Smart Compact Lenses provide a realistic way toward self-powered photonic microsystems enabling embedded biosensing, eye-condition monitoring, and future augmented-reality functionalities.

Keywords: lens, eye, energy, loop antenna, optics.

1. INTRODUCTION

Since their invention by Adolf Gaston Eugen Fick in 1888 [1], contact lenses have primarily been used for vision correction, offering advantages over glasses such as unobstructed peripheral vision, reduced glare and distortion, greater freedom during activities, and no change to appearance. Despite these benefits, they present limitations including infection risks from poor hygiene, dryness or irritation, strict maintenance routines, and adaptation difficulties for some users. Recent advances have led to the development of smart contact lenses (SCLs), which integrate functions such as augmented reality displays and real-time biosensing [2-6]. Studies have demonstrated innovations including scleral lenses with integrated near-infrared lasers that improve eye-tracking reliability and wireless infrared laser pointers enabling beam collimation or image projection for visual assistance. Research also highlights their potential for non-invasive medical monitoring, such as measuring glucose levels or intraocular pressure to aid diseases like Glaucoma, as well as applications in drug delivery and colour-blindness treatment. However, powering microscale electronics within lenses remains a major challenge; proposed solutions include harvesting mechanical energy from blinking or using tear chemistry for electrochemical energy generation, such as enzymatic glucose-based bio-rechargeable batteries or electrochromic systems that monitor glucose through colour changes without external electronics [7-9]. Contact lens design still depends on the type of vision correction required, spherical lenses for myopia or hyperopia, toric lenses for astigmatism, and multifocal lenses for presbyopia, and current research focuses on overcoming technical constraints and identifying suitable energy sources to enable the next generation of autonomous smart contact lenses.

2. SMART CONTACT LENSES: FUNCTIONAL PRINCIPLES

SCLs integrate sensors, communication interfaces, and power circuits into a soft, transparent corneal substrate and support several emerging applications. They enable non-invasive health monitoring by tracking indicators such as glucose levels or intraocular pressure without needles or surgery, using embedded sensors and optical technologies to make medical monitoring safer and more comfortable. SCLs can also enhance vision through augmented perception, providing overlays such as night vision or real-time text translation through AR systems. For visually impaired users, they may improve access to information and assist daily tasks by adjusting lens convergence to support the ciliary muscle responsible for accommodation [10-11].

Advances in manufacturing, including 3D-printed lenses made from biocompatible materials such as PDMS and microfabrication techniques like two-photon polymerization, enable precise and mechanically robust designs with complex microstructures for adaptive optics and responsive visual systems. Their design requires balancing miniaturization, transparency, oxygen permeability, and comfort while integrating components such as antennas, ASICs, and sensors for communication with smart devices and functions like progressive lens orientation. Flexible polymers and nanoscale films are essential to this integration, allowing lenses to detect ocular biomarkers, store energy, transmit data, and potentially deliver drugs, although limited tear exchange in soft lenses remains a challenge that can affect debris removal and measurement accuracy.

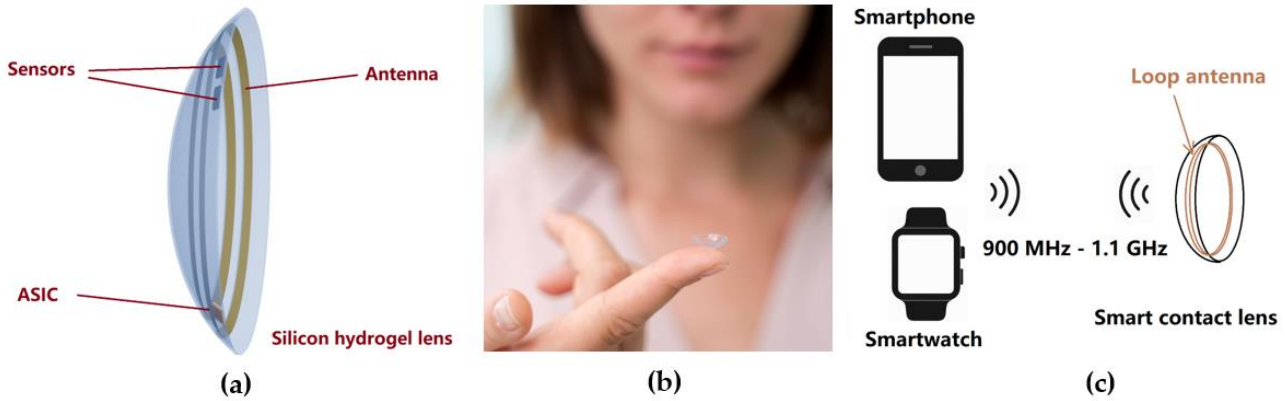

Figure 1. (a) This Figure illustrates the general principle of making a contact lens, which includes an antenna, an application-specific integrated circuit (ASIC), and sensors to communicate with a smartwatch, a mobile phone, or a computer. Technologically, the addition of components in a lens allows, if necessary, to position a progressive contact lens by correctly orienting it. These technologies are feasible. (b) This Photography [12] illustrates the scale and delicacy of a standard contact lens, highlighting the complexity of embedding electronic systems within such a confined space. (c) Illustration of the communication between a smart contact lens and a smartwatch and/or a smartphone. Indicated frequency bandwidth corresponds to what is discussed in [6,13].

3. AUTONOMOUS POWERING VIA EYE-INTRINSIC OR OTHER SOURCES

The development of smart contact lenses (SCLs) is accelerating, driven by bio-compatible electronics and the demand for autonomous wearables. A major challenge is providing safe, efficient, and sustainable power. Emerging strategies include harvesting energy from the body or environment. Tear fluid, rich in electrolytes, can power micro-batteries and biofuel cells. Glucose-coated ultra-thin batteries have shown extended operation, with NTU Singapore demonstrating a 13-hour lens powered solely by tears. Safer alternatives to lithium-ion, like Copper Hexacyanoferrate and Prussian Blue hydrogels, achieve 0.132 mAh capacity while remaining biocompatible. Biomechanical energy from blinking can drive piezoelectric or triboelectric nanogenerators. Hybrid systems combining flexible solar cells with blink-activated Mg–O_2 collectors provide continuous DC power without external accessories, enabling fully autonomous lenses. Other sources include kinetic energy from head or body movement, which can feed microdevices via elastic energy capture. Integrating multiple energy methods into a 10 mm lens requires precise design: a miniaturized energy source, double-loop antenna, low-power ASIC, and multiple sensors must fit compactly while maintaining biocompatibility, oxygen permeability, and user comfort. 3D printing adds complexity, but careful weight distribution ensures self-alignment for vision correction. For more information, see references [14-21].

4. TECHNICAL EXPERTISE AND DESIGN CONSTRAINTS

Developing smart lenses that integrate multiple technologies for visual enhancement or information display is highly complex and requires expertise across optics, materials science, and electronics [6]. Key aspects include thin-film optical coatings, which control light, improve optical quality, and ensure durability in both every day and medical applications; biocompatible materials and compliance with Specific Absorption Rate (SAR) standards [22] to guarantee safe eye contact and efficient wireless signal transfer; signal integrity and frequency analysis to maintain reliable optical and wireless communications (Bluetooth, Wi-Fi, GNSS) while

preventing interference; and careful evaluation of measurement uncertainty to ensure accurate and consistent optical and sensor performance despite manufacturing or environmental variations. In addition, awareness of the patent landscape is essential to protect innovations, avoid infringement, and support funding and commercialization. The convergence of these domains enables the development of energy-autonomous, safe, and manufacturable smart lens prototypes, where successful integration must balance optical performance, electronic functionality, user safety, and signal reliability to achieve a commercially viable product. Additionally we rely on our experiences in frequency [23] and material for optics uncertainty analysis [24-28].

5. OPERATING FREQUENCY RANGE

This section presents the technical characteristics of a compact stacked double loop antenna designed for directional electromagnetic transmission and reception. A loop (or magnetic loop) antenna operates by sensing the magnetic field according to the Lenz–Faraday law, where the induced voltage is proportional to the magnetic flux, placing it in the category of fluxmeters. The structure consists of two vertically aligned circular loops acting as magnetic dipoles, which improves directional radiation for focused transmission or sensing. Each loop has a diameter of 9.5 mm, selected to remain compatible with typical lens dimensions without obstructing vision [13]. According to small loop antenna theory, this geometry corresponds to a resonant frequency near 1.01 GHz and an operating range of approximately 900 MHz–1.1 GHz, suitable for modern communication and detection systems. The radiation pattern is optimized along the vertical axis (broadside to the loop plane), with maximum emission and reception at $\theta = 0°$ and $\theta = 180°$, improving signal gain and targeting precision. This section summarizes the key physical parameters, theoretical considerations, and practical aspects involved in estimating frequency and wavelength, contributing to the understanding of antenna performance and design constraints in the GHz range.

A stacked double loop antenna consists of two circular loops aligned vertically, functioning as magnetic dipoles. This structure is often used for directional emission and reception, behaving like two magnetic dipoles in phase. These antennas are used for directional radiation and reception. For a loop with a 9.5 mm diameter (D = 0.0095 m), the radius is r = D / 2 = 4.75 mm, leading to a loop circumference of approximately $C = 2\pi r = 0.0298$ m. In small loop antenna theory, resonance typically occurs when the circumference is about one-tenth of the wavelength. Thus, the estimated resonant wavelength is 0.298 m. For small loop antennas, the resonant condition typically occurs when the loop circumference is approximately 1/10 of the wavelength (λ). We assume that the loop diameter is D = 9.5 mm. The key criterion for a small loop antenna is: loop circumference C is negligible compared to λ with $\frac{c}{\lambda} < \frac{1}{10}$ (*Equation 1).* Using those formula: $\lambda \approx 10 \times C = 0.298$ m *(Equation 2)*, $f = c / \lambda \approx 3 \times 10^8 / 0.298 \approx 1.01$ GHz *(Equation 3),* and using the speed of light ($c = 3\times10^8$ m/s), the resonant frequency is approximately determined as 1.01 GHz. Given a centered resonant frequency of ~1.01 GHz, the typical usable bandwidth is approximately 900 MHz to 1.1 GHz. Since antennas are reciprocal, they operate similarly for both transmission and reception, that's why the expected operating frequency range for this antenna is in [900 MHz, 1.1 GHz]. The exact usable bandwidth may vary depending on the antenna's Q-factor and matching components. Since antennas are reciprocal, the operating frequency range is the same for both transmission and reception. Given a centered resonant frequency of ~1.01 GHz, the typical usable bandwidth is approximately 900 MHz to 1.1 GHz.

So preferred emission/reception directions are along the axis of the loop stack: $\theta = 0°$ and $\theta = 180°$. This improves directivity and gain in those directions, making the antenna more effective for targeted communication or sensing. When two such loops are stacked, the radiation is reinforced along the axis of the loop stack. Single loop antenna radiates most strongly in the plane perpendicular to its axis. The Q-factor (quality factor) of a small loop antenna is typically estimated as

$$\boldsymbol{Q} \approx \frac{\boldsymbol{f_0}}{\boldsymbol{\Delta f}} \quad \textit{(Equation 4)}$$

Given f0 = 1.01 GHz and $\Delta f = 200$ MHz (-3 dB bandwidth), the estimated Q-factor is approximately as $\boldsymbol{Q} \approx \frac{\boldsymbol{1010}}{\boldsymbol{200}}$. It gives $Q \approx 5.05$. This is very low, which is favorable for wideband operation and suggests the antenna is efficient for communication. We can also roughly estimate the theoretical Q-factor of a small loop antenna

using the radiation resistance Rr and loss resistance Rl:

$$Q = \frac{2\pi fL}{R} \quad (Equation\ 5)$$

However, this requires an estimation of the inductance L of the loop, and knowing or approximating the resistance R. For a single-turn circular loop of radius r, made from a thin conductor, inductance of the loop is:

$$L = \mu_0 r\left[Ln\left(\frac{8r}{a}\right) - 2\right] \quad (Equation\ 6)$$

where r=4.75 mm, wire radius could be a=25 μm, and μ0 = 4π×10−7 H/m. Using this, we can say the inductance is in the nH range, and combined with expected loss resistance of several ohms, a Q-factor of 5 to 10 maximum is typical and reasonable for such compact antennas. It gives L=5.96nH.

6. ELECTRICAL AND THERMAL EFFECTS OF ANTENNAS

The polar plot given in Figure 2 shows the normalized radiation pattern of the loop antenna in the far-field. It's a typical donut-shaped (toroidal) pattern characteristic of small loop antennas, with maximum radiation perpendicular to the plane of the loop and nulls along the axis. Classic small loop pattern proportional to $\sin^2(\theta)$, indicating nulls along the axis of the loop and maximums in the plane of the loop. Radiation pattern of the small loop antenna, showing the classic toroidal shape (donut-like structure) where radiation is strongest in the plane of the loop and nulls occur along the axis perpendicular to the plane. Parameters are summarized in Table 1. Efficiency and frequency bandwidth are given in Figure 3 accordingly.

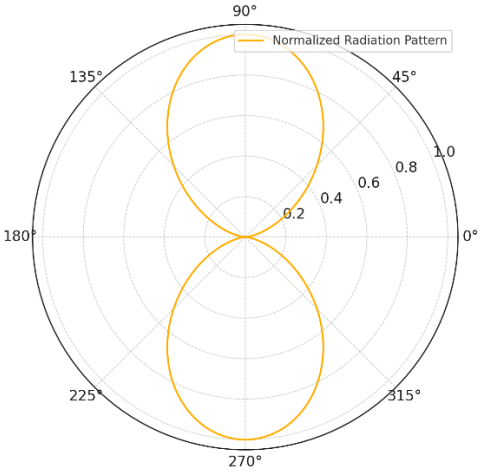

Figure 2. Small double loop antenna of 9.5 mm diameter normalized radiation pattern.

Table 1. Settings for parameters of antennas.

Parameter	Designation	Value (Range)
Hydrogel contact lens diameter	D_L	10 mm
Radius of large loop antenna	r_1	4.75 mm
Radius of smaller loop antenna	r_2	0.95 mm
Wire thickness	2a	50 μm
Wire radius	a	25 μm
Large loop antenna area	A_1	7.09×10^{-5} m²
Smaller loop antenna area	A_2	2.83×10^{-6} m²
Thermal conductivity of Gold	κ	318 W/mK
Electrical resistivity of Gold	ϱ	2.44×10^{-8} Ω·m
Electrical conductivity of Gold	σ_{Au}	4.52×10^{7} S/m
Electrical conductivity of Hydrogel	σ_H	0.3 S/m
Relative permittivity of Hydrogel in 900 – 1100 MHz range GHz	E_H	79
Vacuum permeability	μ_0	$4\pi\times10^{-7}$ H/m

Loop antennas can be analyzed as magnetic dipoles at these sizes (loop << wavelength) [13]. The mutual coupling (inductive) depends on distance and orientation, loop areas, relative position (offset vs. concentric) and mutual inductance M. The coupling coefficient k is given by

$$k = \frac{M}{\sqrt{L_1 L_2}} \quad (Equation\ 7)$$

where M is the mutual inductance and L_1, L_2 are respectively self-inductances of the large and small loops. Self-inductances are estimated as for small single-turn circular loops as in equation 6 relatively to r is the loop radius, a is the wire radius (25 μm) and μ0=4π×10−7 H/m. So, for the larger loop, $L_1 = 5.96$ nH, and for the smaller loop, $L_2 = 4.68$ nH. The coupling coefficient with equation 7 gives k = 0.2. This is moderate to strong coupling, but less than if they were concentric. Results for self-inductances are given in Table 2. Mutual Inductance M can be determined as follow. If the loops were coaxial and centered, we could approximate M using $M = \frac{\mu_0 \cdot (A_1 A_2)}{2\pi \times d^3}$ $(Equation\ 8)$. But since the small loop is placed at the bottom edge of the large loop, mutual coupling is reduced due to non-concentricity. Let's model the reduction using a simplified geometric factor γ, where: $M_{offset} \approx \gamma \cdot M_{centered}$ (*Equation 9*). Typically, for close proximity but off-centered configurations, γ ≈0.3−0.5 depending on distance, we keep the value γ≈0.4. Assuming $A_2 = \pi . r^2 = 2.83.10^{-6} m^2$ and distance between centers d≈r_1−r_2=3.8 mm, then M= $\gamma \cdot 4\pi \times 10^{-7} \cdot [(7.09 \times 10^{-5} \text{ x } 2.83 \times 10^{-6})/(2\pi \times 0.0033^3)$.

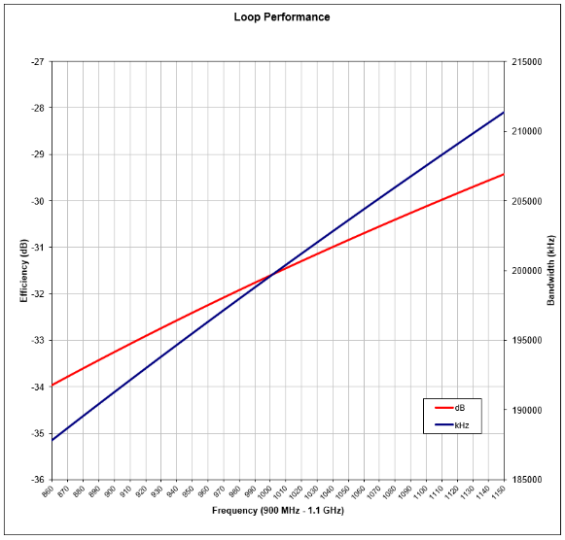

Figure 3. Efficiency (in dB) and frequency bandwidth (expressed in kHz) of the main loop antenna versus frequency expressed in MHz is determined according to the 1.01 GHz centered frequency, 9.5 mm diameter, Gold electrical parameters – see Table 2, and based on the work of. Q-factor is predicted at 5.05 and measured at 4.98.

As illustrated on Figure 4, in reality, we need to extract the microwave signal received by this receiving loop antenna. The classic method is to use inductive coupling, as in transmitting. Optimal coupling (not too tight) allows maximum energy to be extracted. Coupling that is "tighter" than optimal dampens the loop by reducing its gain, selectivity, and quality factor. This is acceptable for shortwave reception because the noise received by the antenna is significantly louder than thermal noise. Variable capacity is to fit the resonance of the larger loop antenna around 1.01 GHz. One of the advantages of this configuration is the following. The output level is not very variable in terms of power between 900 MHz and 1.1 GHz, and the quality factor is not very high, since it is around 5. This means that in practice we will avoid having to adjust the variable capacity all the time after adaptation. Such parameters could be specified in further work. Thermal and Resistive Effects are determined considering materials. Gold is a good conductor, but the antennas are very small, so skin effect and resistive losses are still important at 1.01 GHz. Information concerning skin depth is

given in Table 3. Skin depth is $\delta=\sqrt{((2\rho)/(\mu 0\cdot\omega))}=0.7\mu m$ (Equation 10). So, most current is in outer ~1 μm of wire. $\delta >> 50$ μm, so skin effect is dominant. Effective resistance R increases due to small cross-sectional area and skin effect. This system is highly lossy, and mostly near-field reactive coupling dominates. Coupling coefficient is moderate (~0.59), but effective power transfer is severely limited by losses. Mutual inductance is still appreciable given proximity and loop areas. Radiation from either loop is minimal due to poor radiation efficiency. The off-center small loop decreases M, but not drastically - still strong inductive link. The dominant interaction is near-field magnetic coupling, not far-field radiation. We can summarize the main points. The electromagnetic coupling between these two loops is moderately strong inductively. Offset positioning at the bottom weakens but does not nullify the mutual inductance. Power transfer or re-radiation is heavily limited due to (i) Small loop sizes ($<<\lambda$), (ii) High conductor losses (tiny gold wires, high resistivity at GHz with skin effect), (iii) Very low radiation resistance. This system is suitable for near-field sensing, mutual inductance-based energy transfer, or implantable communication, but not efficient RF transmission. We assume that a smartwatch could be at 80 cm from the antenna and try to estimate the power of the received signal. The double-loop antenna integrated in the smart contact lens operates around 1 GHz and radiates preferentially along the vertical axis ($\theta = 0°$ and 180°), which in principle enables transmission toward a smartwatch positioned about 80 cm away in the same plane. However, this situation is not ideal, since the radiation null of a small loop lies in its plane, meaning that if the watch is not aligned with the vertical radiation lobes, coupling will be very weak. At 80 cm, the separation corresponds to ~2.7 wavelengths ($\lambda \approx 0.3$ m), which is in the radiating (far-field) zone for such a small loop. Given the very low radiation efficiency of the lens antenna ($\eta \approx 0.02\text{-}0.71\%$) [23] and its extremely low radiation resistance ($Rr \approx 0.127\ m\Omega$), the radiated power is several tens of dB lower than the input power delivered by the ASIC. For instance, if the ASIC drives 0 dBm (1 mW) into the antenna, only about 200 nW to 7 μW is actually radiated. The free-space path loss at 1 GHz over 0.8 m is roughly 30 dB, meaning the received signal power at the smartwatch antenna would drop to the range of –90 dBm to –70 dBm depending on efficiency and orientation. While this level could still be detectable with a sensitive receiver, it is close to the limit for robust communication. Potential problems include: strong dependence on antenna orientation (since the smartwatch antenna must be aligned with the vertical radiation lobes), absorption [24] and detuning by the lossy hydrogel and the eye tissue, and high resistive losses due to the skin effect in thin gold conductors. These factors suggest that while communication over 80 cm is possible, in practice the link budget is marginal and would require careful optimization of antenna matching, smartwatch sensitivity, and possibly near-field inductive coupling for shorter, more reliable communication.

To enhance communication between a smart contact lens and a smartwatch, several optimization strategies can be implemented, focusing on antenna performance, receiver sensitivity, and coupling methods. Improving antenna matching and efficiency is essential [29], as adaptive matching networks can compensate for detuning caused by the surrounding eye tissue, while high-conductivity materials and optimized antenna geometries reduce resistive losses and improve radiation resistance; approaches such as high-impedance surfaces have also been shown to enhance impedance matching in wearable antennas. At the receiver side, improving smartwatch sensitivity [30] involves optimizing antenna design to minimize wrist-related effects and refining front-end electronics to reduce noise, with compact dual-band wearable textile antennas demonstrating high gain and efficiency. For short-range links, near-field inductive coupling [31] can provide more reliable and energy-efficient communication than purely radiative methods, particularly when integrated couplers combine near-field communication with wireless power transfer. Overall system performance benefits from a holistic optimization of both the lens and smartwatch components [32], including efficient antenna designs with appropriate radiation patterns, improved receiver sensitivity, and the integration of near-field communication technologies, with emerging nanomaterial-based wearable antennas offering promising opportunities for further improvement.

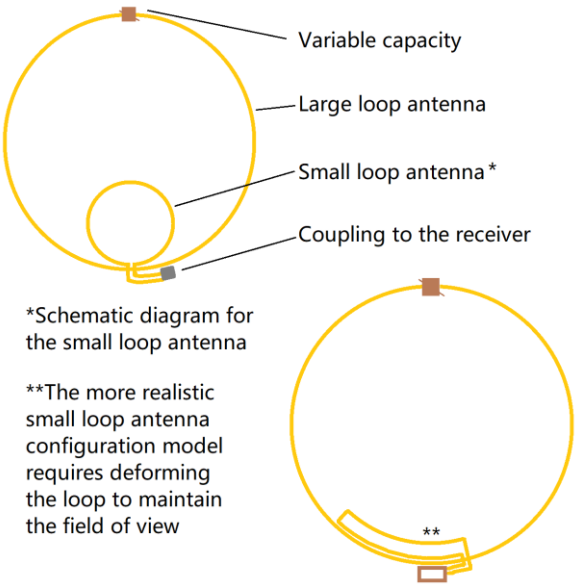

Figure 4. This figure illustrates the problem of coupling to the transmitter-receiver antenna with the need to maintain the field of vision through the lens. Gold loops of the antennas are shown in yellow gold colour. The brown rectangle in the lower right corner symbolizes the ASIC.

7. CONCLUSION

The development of self-powered smart contact lenses represents a convergence of cutting-edge science and engineering, bridging optics, microelectronics, energy harvesting, and biomedical design. By integrating autonomous energy sources such as tear-based biofuel cells, blink-driven nanogenerators, and kinetic harvesters with advanced microfabricated antennas, these lenses move beyond conventional vision correction into multifunctional platforms capable of continuous sensing and communication. The research presented highlights not only the technical feasibility of such systems but also the complexity of balancing miniaturization, transparency, comfort, and biocompatibility. Equally critical are the safety and regulatory dimensions, including compliance with SAR standards and long-term biocompatibility of thin-film coatings. Frequency allocation, signal integrity diagnostics, and uncertainty quantification further underscore the multidisciplinary expertise required to ensure functional reliability. At the same time, awareness of the patent landscape and intellectual property protection will be vital in translating prototypes into scalable, commercially viable products. The promise of smart contact lenses extends well beyond augmented vision, encompassing real-time health monitoring, drug delivery, and adaptive visual aids for patients with chronic conditions or impaired sight. With continued progress in microfabrication, hybrid energy systems, and biosensor integration, smart lenses are poised to become powerful tools at the intersection of healthcare, wearable technology, and human–machine interaction. Ultimately, this work lays the groundwork for a new generation of autonomous, biocompatible, and networked ocular devices that could transform personalized medicine and redefine how humans interact with digital and biological environments.

REFERENCES

[1] Efron N., Pearson R.M., "Centenary celebration of Fick's Eine Contactbrille," Arch. Ophthalmol. 106(10), 1370–1377 (1988). https://doi.org/10.1001/archopht.1988.01060140534019.

[2] Vorobev A.Y., Vorobyev K.A., "History of the emergence and development of smart contact lenses," Cifra. Biomedical Sciences 3(3), 1–10 (2024). https://doi.org/10.60797/BMED.2024.3.3.

[3] Fradkin I.M., Kirtaev R.V., Mironov M.S., Grudinin D.V., Marchenko A.A., Chugunova M.M., Solovey V.R., Xuy A.V., Vyshnevyy A.A., Radko I.P., Arsenin A.V., Volkov V.S., "Contact Lens with Moiré Patterns for High-Precision Eye Tracking," arXiv 2025, arXiv:2505.05147. https://doi.org/10.48550/arXiv.2505.05147.

[4] Shaw S., Nath M., Datta A., Sen S., "Efficient Communication and Powering for Smart Contact Lens with Resonant Magneto-Quasistatic Coupling," arXiv 2024, arXiv:2406.08220. https://doi.org/10.48550/arXiv.2406.08220.

[5] F.-M. Robert et al, "Potential of a laser pointer contact lens to improve the reliability of video-based eye-trackers in indoor and outdoor conditions," Journal of Eye Movement Research, 17(1), 1-16 (2024). https://doi.org/10.16910/jemr.17.1.5.

[6] P. Salzenstein, B. Guichardaz, A. M. Bessou, E. Pavlyuchenko, M. V. Pogumirsky, "Towards self-powered smart contact lenses: integration of autonomous power sources, microfabricated antennas, and multidisciplinary design constraints," Proc. SPIE 13720, Optical Metrology and Inspection for Industrial Applications XII, 137201Q (2025). https://doi.org/10.1117/12.3076622.
[7] Wiemer M., Winoto R., "Mojo Lens-AR contact lenses for real people," Proc. of the 2021 IEEE Hot Chips 33 Symposium (HCS), Palo Alto, CA, USA, 22–24 August 2021, pp. 1–56. https://doi.org/10.1109/HCS52781.2021.9567321.
[8] Jeonghun Yun et al, "A tear-based battery charged by biofuel for smart contact lenses," Nano Energy 110(1), 108344 (2023). https://doi.org/10.1016/j.nanoen.2023.108344.
[9] Zongkang Li et al, "Power-Free Contact Lens for Glucose Sensing," Advanced Functional Materials 33(42), 2304647 (2023). https://doi.org/10.1002/adfm.202304647.
[10] Thiele S., Arzenbacher K., Gissibl T., Giessen H., Herkommer A., "3D-printed eagle eye: Compound microlens system for foveated imaging," Science Advances 3(2), e1602655 (2018+7). https://doi.org/10.1126/sciadv.1602655.
[11] Schmid M., Sterl F., Thiele S., Herkommer A., Giessen H., "3D printed hybrid refractive/diffractive achromat and apochromat for the visible wavelength range," Optics Letters 46(10), 2485-2488 (2021). https://doi.org/10.1364/OL.423196.
[12] Woman checking some new lenses. Designed by Freepik, https://fr.freepik.com/photos-gratuite/femme-verifiant-nouvelles-lentilles_17827515.htm (accessed on 25 March 2026).
[13] P. Salzenstein, A. M. Bessou, L. Salzenstein, "1GHz loop antennas-based smart contact lenses," Proc. SPIE 13720, Optical Metrology and Inspection for Industrial Applications XII, 137200S (2025). https://doi.org/10.1117/12.3076617.
[14] Xiaohu Liu, Ying Ye, Yuancai Ge, Jia Qu, Bo Liedberg, Qingwen Zhang, and Yi Wang, "Smart contact lenses for healthcare monitoring and therapy," ACS Nano 18(9), 6817–6844 (2024). https://doi.org/10.1021/acsnano.3c12072.
[15] Kim J., Cha E., Park J.U., "Recent Advances in Smart Contact Lenses," Adv. Mater. Technol. 5(1), 1900728 (2019). https://doi.org/10.1002/admt.201900728.
[16] Muntz A., Subbaraman L.N., Sorbara L.; Jones L., "Tear exchange and contact lenses: A review," J. Optom. 8(1), 2–11 (2015). https://doi.org/10.1016/j.optom.2014.12.001.
[17] Modic, E.E. "Smart contact lenses powered by micrometers-thin saline-charged batteries," Today's Medical Development 2023. https://www.todaysmedicaldevelopments.com/news/smart-contact-lenese-powered-micrometers-thin-saline-charged-batteries/ (accessed on 25 March 2026).
[18] Neff V.D., "Electrochemical Oxidation and Reduction of Thin Films of Prussian Blue," Journal of The Electrochemical Society 125, 886 (1978). https://doi.org/10.1149/1.2131575.
[19] Pourshaban E., Karkhanis M.U., Deshpande, A., et al., "Power scavenging microsystem for smart contact lenses," Small 2024, 20(32), 2401068. https://doi.org/10.1002/smll.202401068.
[20] Holt K.G., Jeng S.F., Ratcliffe R., Hamill J., "Energetic cost and stability during human walking at the preferred stride frequency," J. Mot. Behav. 27(2), 164–178 (1995). https://doi.org/10.1080/00222895.1995.9941708.
[21] van Ingen Schenau G.J., "An alternative view of the concept of utilisation of elastic energy in human movement," Hum. Mov. Sci. 3(4), 301–336 (1984). https://doi.org/10.1016/0167-9457(84)90013-7.
[22] IEC/IEEE. IEC/IEEE International Standard—Measurement Procedure for the Assessment of Specific Absorption Rate of Human Exposure to Radio Frequency Fields from Hand-Held and Body-Mounted Wireless Communication Devices—Part 1528: Human Models, Instrumentation, and Procedures (Frequency Range of 4 MHz to 10 GHz); IEC/IEEE 62209-1528:2020; IEEE: New York, NY, USA, 2020; pp. 1–284. https://doi.org/10.1109/IEEESTD.2020.9231298.
[23] Salzenstein P., Cholley N., Kuna A., Abbé P., Lardet-Vieudrin F., Sojdr L. and Chauvin J., "Distributed amplified ultra-stable signal quartz oscillator based," Measurement 45(7), 1937–1939 (2012). https://doi.org/10.1016/j.measurement.2012.03.035.
[24] Salzenstein P., Tavernier H., Volyanskiy K., Kim N. N. T., Larger L. and Rubiola E., "Optical mini-disk resonator integrated into a compact optoelectronic oscillator," Acta Physica Polonica A 116(4), 661-663 (2009). https://doi.org/10.12693/APhysPolA.116.661.
[25] Salzenstein P., Wu T. Y., "Uncertainty estimation for the Brillouin frequency shift measurement using a scanning tandem Fabry-Pérot interferometer," Micromachines 14(7), 1429 (2023). https://doi.org/10.3390/mi14071429.
[26] Salzenstein P., Mortier M., Sérier-Brault H., Henriet R., Coillet A., Chembo Y. K., Rasoloniaina A., Dumeige Y., Féron P., "Coupling of high quality factor optical resonators," Physica Scripta, T157, 014024 (2013). http://dx.doi.org/10.1088/0031-8949/2013/T157/014024.
[27] Henriet, R., Salzenstein, P., Ristic, D., Coillet, A., Mortier, M., Rasoloniaina, A., Saleh, K., Cibiel, G., Dumeige, Y., Ferrari, M., Chembo, Y. K., Llopis, O., Féron, P., "High quality factor optical resonators," Physica Scripta, T162, 014032 (2014). http://dx.doi.org/10.1088/0031-8949/2014/T162/014032.
[28] Pavlyuchenko E., Salzenstein, P., "Application of modern method of calculating uncertainty to microwaves and opto-electronics," Laser Optics, Saint Petersburg, Russia, June 30 2014-July 4 (2014). http://dx.doi.org/10.1109/LO.2014.6886449.
[29] Bait-Suwailam MM, I. Labiano I, Alomainy A. Impedance Enhancement of Textile Grounded Loop Antenna Using High-Impedance Surface (HIS) for Healthcare Applications. Sensors. 2020; 20(14):3809. https://doi.org/10.3390/s20143809.
[30] Sharma, D., Kumar, S., Tiwari, R.N. et al. On body and off body communication using a compact wideband and high gain wearable textile antenna. Sci Rep 14, 14493 (2024). https://doi.org/10.1038/s41598-024-64932-6.
[31] Bae H, Park S. Design of an Integrated Near-Field Communication and Wireless Power Transfer Coupler for Mobile Device Applications. Technologies. 2025; 13(5):207. https://doi.org/10.3390/technologies13050207.
[32] Wang C, Zhang N, Liu C, Ma B, Zhang K, Li R, Wang Q, Zhang S. New Advances in Antenna Design toward Wearable Devices Based on Nanomaterials. Biosensors. 2024; 14(1):35. https://doi.org/10.3390/bios14010035.